

2-D modeling of cyanobacterial blooms over time

Chu Chen

May 1, 2019

Abstract Cyanobacterial blooms are worldwide environmental issues associated with eutrophication of water bodies. In this study, I built up a 2-D advection-reaction-diffusion model to quantify how the density of cyanobacteria, the density of zooplankton, and the concentration of dissolved phosphorus evolve. By applying this model to an ideal river with laminar flow, I explained why cyanobacteria density near the bank sometimes appears higher compared to the center of slow-flowing eutrophic rivers. This modeling framework may be refined to serve as a tool to forecast cyanobacterial blooms and to study the effectiveness of different controlling measures.

Keywords cyanobacterial bloom eutrophication advection-reaction-diffusion system

Backgrounds

Nowadays, cyanobacterial blooms are worldwide environmental issues posing great threats to ecosystems and human society. Fertilizer runoff and municipal sewage, among other sources, supply water bodies with a large amount of phosphorus and/or nitrogen (eutrophication), favoring cyanobacteria outgrowth. Presence of a high density of cyanobacteria may alter the physicochemical properties of water bodies (like turbidity, pH, and dissolved oxygen level), which can hugely impact aquatic lives. Some species of cyanobacteria produce 2-methylisoborneol and geosmin, which inflict an earthy taste on fish and drinking water. Certain strains of cyanobacteria may even produce cyanotoxins that are poisonous to human beings and other animals [1].

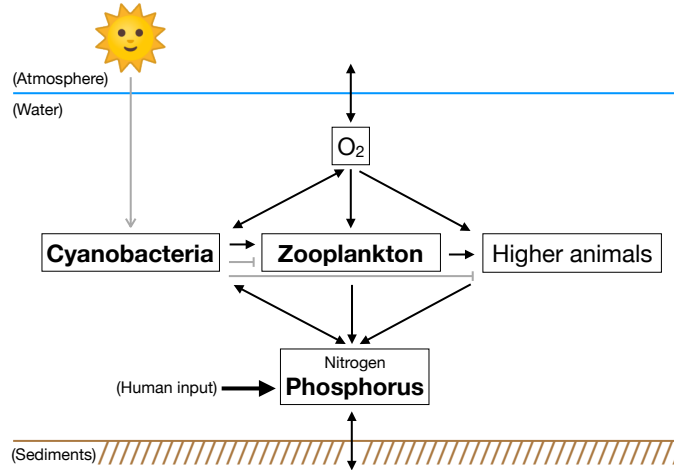


Figure 1. A diagram of main interactions and substance flow between key components of an aquatic ecosystem. Cyanobacteria contribute to dissolved nutrients by decomposition of dead cyanobacteria, excretion of live cyanobacteria, and the nitrogen-fixing activity of certain cyanobacteria species [2]. Decomposition consumes dissolved oxygen [1]. In this study, we will focus on the dynamics of cyanobacteria, zooplankton, and the dissolved limiting nutrient.

A large number of experimental and modeling studies have been performed on different aspects of the mechanics of cyanobacterial blooms. However, most of the modeling studies were based on ordinary differential equations (ODEs) of closed systems developing over time [3, 4]. Very few studies have accounted for fluid dynamics and spatial heterogeneity of realistic water bodies [5, 6].

In this study, I will build up a 2-D partial differential equation (PDE) model to quantify how the density of cyanobacteria, the density of zooplankton, and the concentration of the dissolved limiting nutrient (**Figure 1**) evolve in the presence of advection and diffusion. By applying this model to a river with laminar flow and using finite-difference numerical simulation, I will provide an explanation of why cyanobacteria density near the bank is sometimes higher compared to the center of slow-flowing eutrophic streams.

Models & methods

A river with laminar flow (toy model) Let us consider a river which is straight with a rectangular channel, whose width, slope, and discharge are all constant (**Figure 2**).

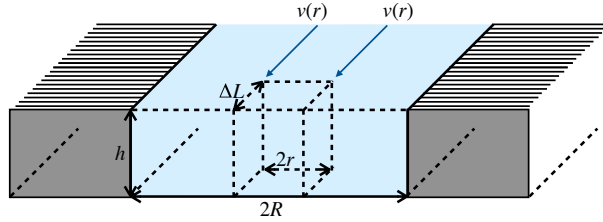


Figure 2. A diagram of the river in the toy model.

Under the condition that flow velocity at a certain point is a function of only the distance r of that point to the center line of the river (*i.e.*, changes across the width of the river but not along its length or depth)

$$|\mathbf{v}| = v(r),$$

the depth h must also not change along the length of the river according to the principle of mass conservation. This condition also implies that the shear stress of water (Newtonian fluid with viscosity μ) is in balance with other forces, including the downstream component of gravity and friction against the bed. The resultant of the gravity component and friction is proportional to the volume (here we designate the coefficient as B). We can write down the force balance equation for a segment of river with width $2r$ (symmetric about the center line of the river) and length ΔL as

$$2\mu v'(r)h\Delta L + 2rh\Delta LB = 0.$$

Therefore,

$$v(r) = -\frac{B}{2\mu}r^2 + C.$$

This indicates that the velocity profile features a parabola, with maximum velocity taken along the center line of the river $v_{\max} = v(0) = C$. Let us designate the width of the river as $2R$ ($0 \leq r \leq R$). Since the flow velocity along the river bank is 0, we have

$$v(R) = -\frac{B}{2\mu}R^2 + v_{\max} = 0,$$

or $v_{\max} = BR^2/(2\mu)$. Substitution of variables yields

$$v(r) = v_{\max}\left(1 - \frac{r^2}{R^2}\right). \quad (1)$$

Turnover-flux equations In this preliminary study on 2-D models, the variability of temperature or sunlight conditions over space or time is not considered. The only environmental factor that affects the growth rate of cyanobacteria is nutrient availability. Here, let us assume that phosphorus is the rate-limiting factor [2]. For simplification, dissolved phosphorus in the environment is treated as a single pool (no compartmentation in particulates). Organic phosphorus in remains and excretions immediately enters this pool and becomes available for assimilation (no necessity of decomposition into phosphate). Exchange with the bottom sedimentation layer is ignored. In addition, only two trophic levels (cyanobacteria and zooplankton) are modeled. The Lotka-Volterra equations (with Holling's Type II functional response, although some filter feeders reportedly feature Type I functional response) are modified to include flux terms [4, 7, 8, 9]. Since little evidence supports the existence of taxis towards cyanobacterial food source for zooplankton as to our knowledge, no such term is incorporated. The resulting governing equations for the density of cyanobacteria B , the density of zooplankton Z , and the concentration of dissolved phosphorus P are

$$\frac{\partial B}{\partial t} = \beta \frac{P}{P + \kappa_P} B - \zeta \frac{B}{B + \kappa_B} Z - \mathbf{v} \cdot \nabla B, \quad (2)$$

$$\frac{\partial Z}{\partial t} = (\epsilon \zeta \frac{B}{B + \kappa_B} - \theta) Z + (D_Z \nabla - \mathbf{v}) \cdot \nabla Z, \quad (3)$$

$$\frac{\partial P}{\partial t} = -\omega \left(\frac{\partial B}{\partial t} + \frac{\partial Z}{\partial t} \right) + (D_P \nabla - \mathbf{v}) \cdot \nabla P. \quad (4)$$

Although pilus-like structures that may facilitate mobility are observed on certain strains of bloom-forming cyanobacteria [10, 11], the fact that they typically clump into colonies during a bloom justifies the omission of a diffusion term in equation (2) above. The meanings and values of parameters in the equations above are listed in **Table 1**.

Table 1. Constant parameters in the turnover-flux equations. β , ω , and κ_P are determined for *Microcystis* sp. An assimilation efficiency ϵ of 0.7 is a consensus in modeling studies. Self-diffusion coefficient of H_2PO_4^- at infinite dilution and 18°C is used as D_P . The effective diffusion coefficient of *Daphnia magna* (a species of water flea) adults at 21 - 23°C is used as D_Z . ζ is the average of measured maximum ingestion rates of *D. magna* at 20°C listed in the citation. Compared to small-bodied zooplankton, large generalist grazers like *Daphnia* are more effective at controlling cyanobacteria [1]. θ is calculated from an average growth yield η of 0.33 concluded in the citation via $\theta = (\epsilon - \eta)\zeta$. κ_B is the average half-saturation constant for grazing of Dinoflagellata, Ciliophora, Rotifera, and Sarcocystophora listed in the citation.

Symbol	Parameter	Value	Reference(s)
β	Maximum cyanobacteria net growth rate	0.045 h^{-1}	[12]
ζ	Maximum zooplankton ingestion rate	0.04 h^{-1}	[13]
ϵ	Assimilation efficiency	0.7	[14]
ω	Phosphorus content in organisms	0.006	[15]
θ	Death (natural/predation) plus excretion and respiration rate of zooplankton	0.015 h^{-1}	[13]
κ_P	Phosphorus concentration at which cyanobacteria net growth rate reaches $\beta/2$	0.015 mg/L	[12]
κ_B	Cyanobacteria density at which zooplankton predation reaches $\zeta/2$	3 mg/L	[16]
D_Z	Effective diffusion coefficient of zooplankton (correlated random walk)	$2.17 \times 10^{-6} \text{ m}^2/\text{s}$	[17, 18]
D_P	Diffusion coefficient of dissolved phosphorus	$7.15 \times 10^{-10} \text{ m}^2/\text{s}$	[19]

The numerical simulation algorithm The river segment in the toy model (with a width of $m\Delta y$ and a length of $n\Delta x$) is discretized into a 2-D matrix $\mathbf{A} = (a_{ij}) \in \mathbb{R}^{m \times n}$. It flows from left to right. Each element a_{ij} represents a tile with an area of $\Delta x \cdot \Delta y$ whose center is $d_i = |(i - 1/2)\Delta y - m\Delta y/2|$ away from the center axis of the river and $l_j = (j - 1)\Delta x$ downstream from the starting line (the line crossing the centers of tiles represented by the first column and subject to the Dirichlet boundary condition). Each tile has 3 properties: the density of cyanobacteria $B_{ij}(t)$, the density of zooplankton $Z_{ij}(t)$, and the concentration of dissolved phosphorus $P_{ij}(t)$. Initial conditions are set to be $\mathbf{a}_{ij}(0) = (B_{ij}(0), Z_{ij}(0), P_{ij}(0)) = (0, 0, 0)$ for all $j > 1$ and i . The steady-state matrix is approximated by allowing the system to develop for a duration of time sufficient for the slowest streamlines (ones along the first and last rows) to travel 3 times the length of the river segment. This entire simulation is discretized into time steps of Δt and looped through the following routine:


- (i) Reset the Dirichlet boundary condition \mathbf{a}_{i1} ;
- (ii) Advect via $\mathbf{a}_{ij}(n\Delta t) := ([\hat{j}] - \hat{j} + 1) \cdot \mathbf{a}_{i[\hat{j}]}((n-1)\Delta t) + (\hat{j} - [\hat{j}]) \cdot \mathbf{a}_{i([\hat{j}] + 1)}((n-1)\Delta t)$, where $\hat{j} := j - v(d_i)\Delta t / \Delta x$ and $v(d_i)$ is calculated using equation (1);
- (iii) Diffuse in 2-D using the alternating direction implicit method [20];
- (iv) Develop \mathbf{a}_{ij} according to **the turnover equations**:

$$\begin{aligned}\frac{dB}{dt} &= \beta \frac{P}{P + \kappa_P} B - \zeta \frac{B}{B + \kappa_B} Z, \\ \frac{dZ}{dt} &= (\epsilon \zeta \frac{B}{B + \kappa_B} - \theta) Z, \\ \frac{dP}{dt} &= -\omega \left(\frac{dB}{dt} + \frac{dZ}{dt} \right),\end{aligned}$$

using the Runge-Kutta method (while keeping the total phosphorus level within each tile conserved).

Numerical simulation codes are written in MATLAB[®] and publicly accessible at <https://github.com/CreLox/CyanobacteriaBloom>.

Results

Linear stability analysis of the turnover equations Let us first investigate the turnover equations (ODEs without the diffusion term or the advection term) and examine the fixed points of this time-invariant system using linear stability analysis. It should be noted that as cited in [3], fixed points and their stability might behave differently with the presence of the diffusion terms, as well as numerical errors introduced during the simulation. 

All fixed points reside on 3 curves in the (B, Z, P) space: $(0, 0, P)$ and $(B, 0, 0)$ represent scenarios where either zooplankton or cyanobacteria die out, with the non-degenerate ones being:

$$\left(\frac{\theta}{\epsilon \zeta - \theta} \kappa_B, \frac{\beta \epsilon}{\epsilon \zeta - \theta} \frac{P}{P + \kappa_P} \kappa_B, P \right). \quad (5)$$

The Jacobian matrix of these autonomous ODEs is

$$\mathbf{J} = \begin{bmatrix} \frac{\beta P}{P + \kappa_P} - \frac{\zeta \kappa_B Z}{(B + \kappa_B)^2} & -\frac{\zeta B}{B + \kappa_B} & \frac{\beta \kappa_P B}{(P + \kappa_P)^2} \\ \frac{\epsilon \zeta \kappa_B Z}{(B + \kappa_B)^2} & \frac{\epsilon \zeta B}{B + \kappa_B} - \theta & 0 \\ -\frac{\omega \beta P}{P + \kappa_P} + \frac{\omega(1 - \epsilon) \zeta \kappa_B Z}{(B + \kappa_B)^2} & \frac{\omega(1 - \epsilon) \zeta B}{B + \kappa_B} + \omega \theta & -\frac{\omega \beta \kappa_P B}{(P + \kappa_P)^2} \end{bmatrix}.$$

(i) When evaluated along $(0, 0, P)$, \mathbf{J} becomes

$$\begin{bmatrix} \frac{\beta P}{P + \kappa_P} & 0 & 0 \\ 0 & -\theta & 0 \\ -\frac{\omega \beta P}{P + \kappa_P} & \omega \theta & 0 \end{bmatrix},$$

which indicates that $(0, 0, P)$ is not stable since $\beta P / (P + \kappa_P) > 0$ (note that this system will never reach $(0, 0, 0)$ if initially not all of B, P, Z are 0, given that the total phosphorus level in the system $P + \omega(B + Z)$ is conserved).

(ii) When evaluated along $(B, 0, 0)$, \mathbf{J} becomes

$$\begin{bmatrix} 0 & -\frac{\zeta B}{B + \kappa_B} & \frac{\beta B}{\kappa_P} \\ 0 & \frac{\epsilon \zeta B}{B + \kappa_B} - \theta & 0 \\ 0 & \frac{\omega(1 - \epsilon)\zeta B}{B + \kappa_B} + \omega \theta & -\frac{\omega \beta B}{\kappa_P} \end{bmatrix}.$$

The fixed-point stability depends on the sign of $\epsilon \zeta B / (B + \kappa_B) - \theta$. If $B < \theta \kappa_B / (\epsilon \zeta - \theta)$, $(B, 0, 0)$ will be a stable fixed point (the cyanobacteria biomass cannot support the growth of a small population of zooplankton being introduced). If $B > \theta \kappa_B / (\epsilon \zeta - \theta)$, $(B, 0, 0)$ will be unstable. Let us designate the threshold as $\hat{B} := \theta \kappa_B / (\epsilon \zeta - \theta)$. Using the values listed in **Table 1**, we calculate $\hat{B} \approx 3.4 \text{ mg/L}$. As a straightforward corollary, if the total phosphorus level in the system is greater than $\omega \hat{B} \approx 0.020 \text{ mg/L}$, the system will never reach or stably stay at $(B, 0, 0)$.

(iii) To evaluate the stability of fix points shown in formula (5), let us first rewrite the ODEs by eliminating P , using the conservation of phosphorus $P + \omega(B + Z) \equiv C$ (where C is a constant determined by initial conditions):

$$\begin{aligned} \frac{dB}{dt} &= \beta \frac{C - \omega(B + Z)}{C - \omega(B + Z) + \kappa_P} B - \zeta \frac{B}{B + \kappa_B} Z, \\ \frac{dZ}{dt} &= (\epsilon \zeta \frac{B}{B + \kappa_B} - \theta) Z. \end{aligned}$$

The new Jacobian matrix is

$$\mathbf{J}^* = \begin{bmatrix} \frac{\beta P}{P + \kappa_P} - \frac{\beta \omega \kappa_P B}{(P + \kappa_P)^2} - \frac{\zeta \kappa_B Z}{(B + \kappa_B)^2} & -\frac{\beta \omega \kappa_P B}{(P + \kappa_P)^2} - \frac{\zeta B}{B + \kappa_B} \\ \frac{\epsilon \zeta \kappa_B Z}{(B + \kappa_B)^2} & \frac{\epsilon \zeta B}{B + \kappa_B} - \theta \end{bmatrix}.$$

When evaluated on formula (5), \mathbf{J}^* becomes

$$\begin{bmatrix} \frac{\beta \theta}{P + \kappa_P} \left(\frac{P}{\epsilon \zeta} - \frac{\omega \kappa_P \kappa_B}{(\epsilon \zeta - \theta)(P + \kappa_P)} \right) & -\frac{\beta \omega \theta \kappa_P \kappa_B}{(\epsilon \zeta - \theta)(P + \kappa_P)^2} - \frac{\theta}{\epsilon} \\ \frac{\beta(\epsilon \zeta - \theta)P}{\zeta(P + \kappa_P)} & 0 \end{bmatrix}.$$

Eigenvalues of the 2×2 matrix \mathbf{J}^* are the solutions of the following equation

$$\lambda^2 - \text{tr}(\mathbf{J}^*) \cdot \lambda + |\mathbf{J}^*| = 0 \quad (6)$$

For $P > 0$, we have $|\mathbf{J}^*| > 0$. According to Vieta's formulas, if equation (6) has 2 real solutions, their signs will be the same as $\text{tr}(\mathbf{J}^*)$. However, if equation (6) has 2 imaginary solutions, their real parts will be $\text{tr}(\mathbf{J}^*)/2$. Therefore, if $(P + \kappa_P)P < \epsilon\omega\kappa_P\kappa_B/\eta$, the fixed point is stable; if $(P + \kappa_P)P > \epsilon\omega\kappa_P\kappa_B/\eta$, the fixed point is unstable. This threshold dissolved phosphorus concentration is about 0.0176 mg/L, which corresponds to a total phosphorus level of about 0.0609 mg/L.

The turnover equations preserve non-negativity Obviously, the density/concentration of cyanobacteria, zooplankton, and dissolved phosphorus will never go below 0. We next prove that the ODE system presented here is self-consistent: for initial conditions $B(0), Z(0), P(0) \geq 0$, we have $\forall t \geq 0, B(t), Z(t), P(t) \geq 0$.

Proof. As long as $B > -\kappa_B$ and $P > -\kappa_P$, the solution can be locally prolonged. Therefore, all we need to prove is that no such $t > 0$ exists that one of $B(t)$, $Z(t)$, and $P(t)$ becomes less than 0 for initial conditions $B(0), Z(0), P(0) \geq 0$.

Otherwise, set $S := \{T \geq 0 | \forall t \in [0, T], B(t), Z(t), P(t) \geq 0\}$ is nonempty ($0 \in S$) and bounded. Let us designate $t_0 := \sup S$. The solution can be prolonged to $t = t_0$ and based on continuity, $B(t_0), Z(t_0), P(t_0) \geq 0$ and at least one of $B(t_0), Z(t_0), P(t_0)$ is 0. With the conservation of $P + \omega(B + Z)$, we can easily show that $\mathbf{f}(B, Z, P) := (dB/dt, dZ/dt, dP/dt)$ is locally Lipschitz continuous near $(B(t_0), Z(t_0), P(t_0))$. According to Picard's Existence and Uniqueness Theorem, whichever (B, Z, P) is 0 at $t = t_0$ must remain 0 in a right neighborhood $[t_0, t_0 + \tau], \tau > 0$. This contradicts the supremum definition. \square

Numerical simulations on the toy model Cyanobacterial blooms in slow-flowing eutrophic rivers tend to be more severe near the bank (**Figure 3**). We next use our model to examine this phenomenon. In the following simulations, the grid size is $0.5\text{ m} \times 0.5\text{ m}$ and each time step is 0.5 h. The scale of the river segment is $50\text{ m} \times 1000\text{ m}$. All tiles along the starting line are set to have the same cyanobacteria density, zooplankton density, and dissolved phosphorus concentration. This setting can be justified by the fact that in reality, upper rivers are usually narrow, fast-flowing, and well-mixed horizontally.



Figure 3. A cyanobacterial bloom in St. Lucie Canal near Indiantown Airport, Florida, on June 8, 2018 (Eric Hasert/TCPalm). Cyanobacteria density appeared higher near the bank.

We will test 3 different boundary conditions here (**Figures 4-6**). In the first scenario, the boundary conditions are set so that the cyanobacteria density cannot support the existence of zooplankton (see part (ii) of the linear stability analysis). As we can see from **Figures 4**, zooplankton density gradually decreases down the river (more steeply near the bank). In the second scenario, the boundary conditions are set to have a higher total phosphorus concentration (above the supporting threshold of zooplankton) compared to the first scenario, by the addition of extra dissolved phosphorus (from 0.01 mg/L to 0.1 mg/L). As we can see from **Figures 5**, zooplankton density indeed increases down the river (again more steeply near the bank).

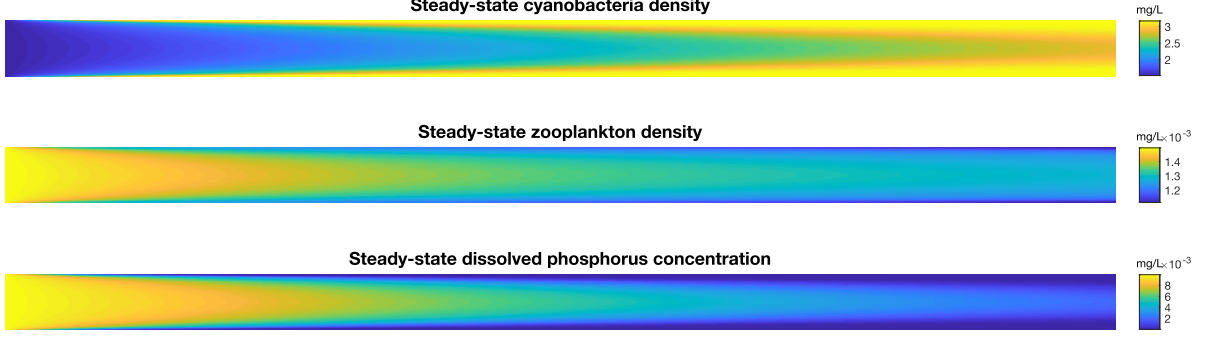


Figure 4. Steady-state colormap of the river with boundary conditions that cannot sustain zooplankton along the starting line. The boundary cyanobacteria density, zooplankton density, and dissolved phosphorus concentration are 1.5 mg/L, 0.0015 mg/L, and 0.01 mg/L, respectively. v_{\max} is set to be 5 mm/s.

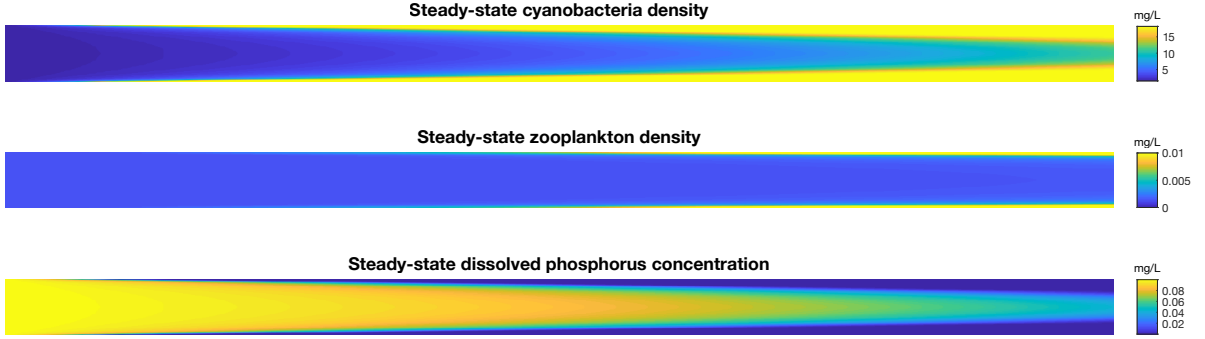


Figure 5. Steady-state colormap of the river with boundary total phosphorus level above the threshold to sustain zooplankton along the starting line. The boundary cyanobacteria density, zooplankton density, and dissolved phosphorus concentration are 1.5 mg/L, 0.0015 mg/L, and 0.1 mg/L, respectively. The colorbar of zooplankton density is adjusted and does not cover the entire data range for better visualization. v_{\max} is set to be 5 mm/s.

The contours are nearly parabolic. This can be explained qualitatively as followed. If we do not consider the diffusion terms (which are actually somewhat insignificant compared to the scale of the river), each streamline (row of the matrix) is independent. We can then define a phase parameter $\phi_{ij} = l_j/v(d_i)$ based on advection. With the boundary conditions that all tiles along the starting line have the same status $(B(0), Z(0), P(0))$, tiles with the same phase ϕ should have the same status $(B(\phi), Z(\phi), P(\phi))$. Because the velocity profile is parabolic (equation 1), the patterns naturally resemble parabolas. This also explains the phenomenon that cyanobacteria density is usually higher near the bank of eutrophic, near-quiescent rivers. Water along the bank has a longer retention time in the channel, and cyanobacteria flowing downstream have more time to utilize rich nutrients to proliferate. ▾

In the third scenario, we verify the stability of the non-degenerate fixed point [formula (5); part (iii) of the linear stability analysis]. The boundary status is set to be $(B(0), Z(0), P(0)) = (3.3636, 3.5795, 0.0150)$ mg/L. The rounding errors serve as a tiny disturbance. As shown in **Figure 6**, the cyanobacteria density, zooplankton density, and dissolved phosphorus concentration are almost homogeneous within the river segment and features phase oscillation (with decreasing amplitudes as phase increases) around the fixed point.

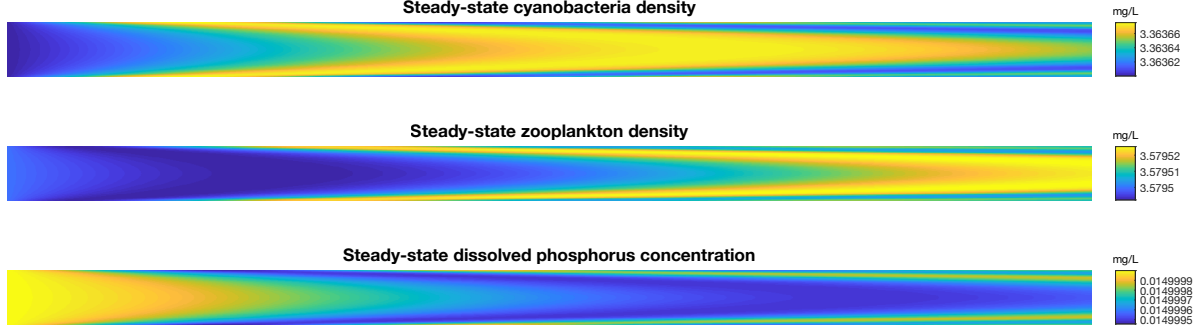


Figure 6. Steady-state colormap of the river with boundary conditions set to be at the non-degenerate fixed point along the starting line. A dissolved phosphorus concentration of 0.0150 mg/L is substituted into formula (5), which is below the threshold and therefore corresponds to a stable fixed point according to the linear stability analysis. v_{\max} is set to be 1 mm/s.

Discussions

Other factors may contribute to the aforementioned phenomenon as well. Near the bank, water is usually warmer in the summer, which facilitates the metabolism and proliferation of cyanobacteria. Irregular bank shapes bays of various sizes, within which water has a long retention time. A realistic non-quiescent water body features chaotic turbulence. The macroscopic consequence of this continuous internal disturbance is the tendency of the system to minimize its mechanical energy. Thus, particles with density higher than that of water appear to be pushed towards slow-flowing regions of the water body. Non-point sources of nutrients (fertilizer runoff and exchange with groundwater [21]) can also enter the river along the bank or through the bed. Furthermore, the physiology of some cyanobacteria species is reportedly affected by hydrodynamics [22].

This finite-difference modeling framework, together with the Lattice Boltzmann method [23] for steady-state flux calculation, should enable cyanobacterial bloom forecast in real lakes based on their precise geometry and inlet/outlet information (locations and discharge). Large freshwater lakes are ecologically and socioeconomically critical, with correlated remote sensing (for quantification of cyanobacteria density [24]), discharge, and water quality data available. In this realistic turbulent environment and at such scale, the model will need to include extra turbulent diffusion terms, while molecular diffusivity and active movement of zooplankton may be ignored depending on the way of discretization.

Previous studies display a large discrepancy on some of the parameter values, which may even vary in the order of magnitude [12]. This hampers reliable modeling studies. Comparing simulations with historic cyanobacterial blooms will help to refine our current model and its parameters, although the algorithm presented here may have to be optimized first to allow for simulations at such scales with reasonable spatial/temporal resolutions.

References

- [1] Michael F. Chislock et al. “Eutrophication: Causes, Consequences, and Controls in Aquatic Ecosystems”. In: *Nature Education Knowledge* 4.4 (2013), p. 10.
- [2] David W. Schindler et al. “Eutrophication of lakes cannot be controlled by reducing nitrogen input: Results of a 37-year whole-ecosystem experiment”. In: *PNAS* 105.32 (2008), pp. 11254–11258.
- [3] John H. Steele and Eric W. Henderson. “The role of predation in plankton models”. In: *Journal of Plankton Research* 14.1 (1992), pp. 157–172.

- [4] Gabriela Elena Dumitran and Liana Ioana Vuta. “Study on Lake Izvorul Muntelui rehabilitation”. In: *Simulation Modelling Practice and Theory* 19.4 (2011), pp. 1235–1242.
- [5] Göran Broström. “On advection and diffusion of plankton in coarse resolution ocean models”. In: *Journal of Marine Systems* 35.1–2 (2002), pp. 99–110.
- [6] Jiantao Zhao, Jianjun Paul Tian, and Junjie Wei. “Minimal Model of Plankton Systems Revisited with Spatial Diffusion and Maturation Delay”. In: *Bulletin of Mathematical Biology* 78.3 (2016), pp. 381–412.
- [7] C. S. Holling. “The Components of Predation as Revealed by a Study of Small-Mammal Predation of the European Pine Sawfly”. In: *The Canadian Entomologist* 91.5 (1959), pp. 293–320.
- [8] Jonathan M. Jeschke, Michael Kopp, and Ralph Tollrian. “Consumer-food systems: why type I functional responses are exclusive to filter feeders”. In: *Biological Reviews* 79.2 (2004), pp. 337–349.
- [9] Jiantao Zhao, Jianjun Paul Tian, and Junjie Wei. “Minimal Model of Plankton Systems Revisited with Spatial Diffusion and Maturation Delay”. In: *Bulletin of Mathematical Biology* 78.3 (2016), pp. 381–412.
- [10] Kenlee Nakasugi and Brett A. Neilan. “Identification of Pilus-Like Structures and Genes in *Microcystis aeruginosa* PCC7806”. In: *Applied and Environmental Microbiology* 71.11 (2005), pp. 7621–7625.
- [11] B. T. M. Mulling, S. A. Wood, and D. P. Hamilton. “Intra-colony motility of *Microcystis wesenbergii* cells”. In: *New Zealand Journal of Botany* 52.1 (2014), pp. 153–159.
- [12] Ming-Ming Ou et al. “Effects of Iron and Phosphorus on *Microcystis* Physiological Reactions”. In: *Biomedical and Environmental Sciences* 19 (2006), pp. 399–404.
- [13] Per Juel Hansen, Peter Koefoed Bjørnsen, and Benni Winding Hansen. “Zooplankton grazing and growth: Scaling within the 2-2,000- μm body size range”. In: *Limnology and Oceanography* 42.4 (1997), pp. 687–704.
- [14] M. R. Landry et al. “Effect of food acclimation on assimilation efficiency of *Calanus pacificus*”. In: *Limnology and Oceanography* 29.2 (1984), pp. 361–364.
- [15] S. Enríquez, C. M. Duarte, and K. Sand-Jensen. “Patterns in decomposition rates among photosynthetic organisms: the importance of detritus C:N:P content”. In: *Oecologia* 94 (1993), pp. 457–471.
- [16] Christian Mulder and A. Jan Hendriks. “Half-saturation constants in functional responses”. In: *Global Ecology and Conservation* 2 (2014), pp. 161–169.
- [17] Niko Komin, Udo Erdmann, and Lutz Schimansky-Geier. “Random walk theory applied to *Daphnia* motion”. In: *Fluctuation and Noise Letters* 4.1 (2004), pp. L151–L159.
- [18] Ricardo Garcia et al. “Optimal foraging by zooplankton within patches: The case of *Daphnia*”. In: *Mathematical Biosciences* 207 (2007), pp. 165–188.
- [19] Yuan-Hui Li and Sandra Gregory. “Diffusion of ions in sea water and in deep-sea sediments”. In: *Geochimica et Cosmochimica Acta* 38 (1974), pp. 703–714.
- [20] Bernard Bialecki and Ryan I. Fernandes. “Orthogonal spline collocation Laplace-modified and alternating-direction methods for parabolic problems on rectangles”. In: *Mathematics of Computation* 60.202 (1993), pp. 545–573.
- [21] Joseph L. Domagalski and Henry M. Johnson. “Subsurface transport of orthophosphate in five agricultural watersheds, USA”. In: *Journal of Hydrology* 409 (2011), pp. 157–171.
- [22] Yang Song et al. “Mechanism of the influence of hydrodynamics on *Microcystis aeruginosa*, a dominant bloom species in reservoirs”. In: *Science of the Total Environment* 636 (2018), pp. 230–239.
- [23] P. L. Bhatnagar, E. P. Gross, and M. Krook. “A Model for Collision Processes in Gases. I. Small Amplitude Processes in Charged and Neutral One-Component Systems”. In: *Physical Review* 94.3 (1954), pp. 511–525.
- [24] Guoqing Wang et al. “Retrieving absorption coefficients of multiple phytoplankton pigments from hyperspectral remote sensing reflectance measured over cyanobacteria bloom waters”. In: *Limnology and Oceanography: Methods* 14.7 (2016), pp. 432–447.

Appendix: Q & A

Q: Can you use this to model other types of bacteria as well?

Q: How would the rate of eutrophication change for a body of freshwater, such as Lake Erie, versus for a body of salt water (e.g. Long Island Sound)? What would have to be changed in your model?

A: This model can simulate cyanobacteria blooms dominated by any species, not just *Microcystis aeruginosa*. The only things that need to be changed are the parameter values.

Q: Would it be helpful to scale this model up to 3D?

A: It can be more realistic but will be much more complicated. In the summer, the upper mixing layer is usually about 10m, which means that shallow water bodies can be modeled just by this 2-D model (see another question below).

Q: How does the width of the canal affect your model?

A: It will change the role that diffusion may potentially play.

Q: If 1 km of a river was very computationally expensive, how long do you predict your whole lake will take to simulate?

A: Currently, the computation complexity scales linearly with the area mn for advection and turnover. Diffusion uses the ADI method which involves matrix multiplication, whose dimension is up to $\max(m, n)^2$.

Q: How do you deal with/incorporate different shapes, sizes, and depths of bodies of water? How much does this affect growth?

A: The Lattice Boltzmann Method can handle any shape as long as we properly set up the grid and specify the boundaries. Depth will be hard to account for in this 2-D model (see another question below). How this may affect the cyanobacteria bloom cannot be predicted without doing the simulation on a case-by-case basis.

Q: Would the flow in a lake be strong enough that you would expect the same/as strong of patterns as in a river?

A: The key is not the velocity but the retention time. The bloom pattern may be very different and has to be analyzed on a case-by-case basis.

Q: Could water depth be accounted for without necessarily converting to a 3D model (total biomass could scale non-linearly with depth; Depth could affect the presence of macroscopic plants on the bottom; flow rates might also be affected by the depth)?

A: It is possible if we do not consider the vertical heterogeneity. We can write down the original conservation equations where we have terms like $\partial(Bh)/\partial t = \dots$ on the left side (h is the local depth). However, if we have to consider the vertical heterogeneity, we will probably need a 3-D model.

Q: Fish (or other macroscopic animals) growth might be on too slow of a timescale to affect the rest of the ecosystem, but fish death/migration might still play a significant role even on a short timescale (there is no limit on the rate of death of fish due to lack of oxygen or toxin presence). Is it reasonable to exclude macroscopic animals from the model?

A: This is a good point. The main reason I omitted them is that a lot of environmental cues will affect their movement (mainly taxis towards oxygen and food, but not advection or diffusion) and are hard to quantify. Also, not all cyanobacteria bloom produce cyanotoxins and even for those that do produce toxins, there are not enough quantitative physiology studies on the metabolisms of their production and toxicity. This model, at its current state, is not meant to include everything - I only use it to explain a specific natural phenomenon.

Q: Is it reasonable to model the movement of cyanobacteria and phosphorus as diffusion due to Brownian motion? Would random small currents in the body of water not far exceed the effect of Brownian motion on the speed of dispersal? This could still be modeled as a random walk/diffusion, but the parameters might need to be adjusted. Additionally, turbulence would affect this rate of small random flows.

Q: Such turbulent mixing of the water column as described above might also have a positive effect on the homogeneity of the water, and affect the growth rates of cyanobacteria and plankton, both due to better mixing of nutrients and turbulence increasing the amount of dissolved oxygen. Could average turbulence be somehow approximated on a large scale without doing fluid simulations?

A: For the two questions above: the assumption of the toy model is laminar flow without disturbance. The goal of this model is not to be as realistic as possible at this stage. Turbulent diffusion is discussed in the paper.

Q: Can you perturb your system at all to see how it affects growth?

A: I tested different boundary conditions in the paper.

Q: Is it possible to evaluate the effects of traditional control measures for eutrophication such as introducing certain fish species, using some chemicals by this model? Or could this model indicate other potential methods to control cyanobacteria blooms?

A: Technically yes, by changing boundary conditions and/or parameters related to growth and death. However, this is not the main interest of this paper.

Q: It was not super clear to me what parts of the model were based on previous work and what were your personal contributions. Can you explain this further?

A: The PDEs here in this paper were not directly from a single paper. Nor was the algorithm. I did the analytical overview and wrote the codes from scratch. The parameters were taken from different papers by careful literature research and comparison. The main phenomenon being studied here has also not been quantitatively studied before. In many ways, this study is brand new.

Q: You mentioned the Lattice Boltzmann Method (LBM) at the very end, what is this model and what does it incorporate? Where is it lacking and what are you adding to make it more accurate?

A: LBM is an algorithm of computational fluid dynamics compatible with the finite-difference framework in this study. It can be used to calculate steady-state flux in realistic water bodies. Its accuracy depends on how the system is discretized.

Q: How are you planning on improving the algorithm (ideally what would you do to improve the algorithm)?

A: I think the diffusion algorithm is the one that has the greatest potential for improvement. However, I have no idea how to improve it significantly for now.

Q: What are the stability and local truncation error of your finite difference method? Why is it the best choice for your system?

A: It may not be the best framework for realistic water bodies with complex shapes but it is the most convenient one for my toy model. The advection algorithm will induce a numerical diffusion artifact. The Runge-Kutta method is a relatively accurate method for solving ODE but it still produces numerical errors. A complete, systematic examination on the numeric error is beyond my ability for now.